Accepted Manuscript

Thigh-calf contact parameters for six high knee flexion postures: Onset, maximum angle, total force, contact area, and center of force.

David C. Kingston, Stacey M. Acker

PII: S0021-9290(17)30674-7
DOI: https://doi.org/10.1016/j.jbiomech.2017.11.022
Reference: BM 8470

To appear in: *Journal of Biomechanics*

Accepted Date: 22 November 2017

Please cite this article as: D.C. Kingston, S.M. Acker, Thigh-calf contact parameters for six high knee flexion postures: Onset, maximum angle, total force, contact area, and center of force., *Journal of Biomechanics* (2017), doi: https://doi.org/10.1016/j.jbiomech.2017.11.022

Original Article

Title:

Thigh-calf contact parameters for six high knee flexion postures: Onset, maximum angle, total force, contact area, and center of force.

Running Title:

Thigh-calf contact parameters of high knee flexion postures.

Authors:

David C Kingston[1]

Stacey M Acker[1]

[1] Department of Kinesiology, University of Waterloo

Corresponding author:

Stacey M. Acker, Department of Kinesiology, University of Waterloo, 200 University Ave W, Waterloo, Ontario, N2L 3G1, Canada; phone (519) 888-4567 ext. 31338; E-Mail: stacey.acker@uwaterloo.ca.

Keywords:

Thigh-calf contact, kneeling, squatting, pressure

Word Count:

3631

Abstract: (max 250)

In high knee flexion, contact between the posterior thigh and calf is expected to decrease forces on tibiofemoral contact surfaces, therefore, thigh-calf contact needs to be thoroughly characterized to model its effect. This study measured knee angles and intersegmental contact parameters in fifty-eight young healthy participants for six common high flexion postures using motion tracking and a pressure sensor attached to the right thigh. Additionally, we introduced and assessed the reliability of a method for reducing noise in pressure sensor output. Five repetitions of two squatting, two kneeling, and two unilateral kneeling movements were completed. Interactions of posture by sex occurred for thigh-calf and heel-gluteal center of force, and thigh-calf contact area. Center of force in thigh-calf regions was farther from the knee joint center in females, compared to males, during unilateral kneeling (82 and 67 mm respectively) with an inverted relationship in the heel-gluteal region (331 and 345 mm respectively), although caution is advised when generalizing these findings from a young, relatively fit sample to a population level. Contact area was larger in females when compared to males (mean of 155.61 and 137.33 cm^2 across postures). A posture main effect was observed in contact force and sex main effects were present in onset and max angle. Males had earlier onset (121.0º) and lower max angle (147.4º) with onset and max angles having a range between movements of 8º and 3º respectively. There was a substantial total force difference of 139N between the largest and smallest activity means. Force parameters measured in this study suggest that knee joint contact models need to incorporate activity-specific parameters when estimating loading.

1. Introduction

The magnitude and location of contact forces between thigh-calf and heel-gluteal structures during high knee flexion postures are critical parameters for understanding knee joint loading. In this study, high knee flexion postures are defined as exceeding 120º flexion (Kingston et al., 2016; Zelle et al., 2009). Given the increased incidence of degenerative knee diseases in populations that regularly assume high knee flexion postures (Baker et al., 2003; Bombardier et al., 2011; Kirkeshov Jensen, 2008), further study to refine potential initiating mechanisms is warranted. A leading theoretical injury mechanism for high knee flexion postures—the exposure of under-conditioned tissues to high joint contact forces (Andriacchi et al., 2004; Andriacchi and Favre, 2014)—does not consider the unloading effect of thigh-calf or heel-gluteal contact on the joint. Therefore, the limited *in vitro* data available from testing knee joint compressive forces, up to 135º of flexion, are likely over-estimates (Hofer et al., 2012; Victor et al., 2009). This potential for over-estimation was first supported by Zelle et al. (2009), who used a finite element model of the knee with external thigh-calf contact forces (taken from Zelle et al. (2007) *in vivo* data). Decreases from 4.37 to 3.07 times body weight (BW) in knee joint compression and 1.31 to 0.72 times BW in shear during a flatfoot squat movement were estimated (Zelle et al., 2009). However, accurate magnitude and location data are critical to improve estimates of joint contact forces in future computational models and *in vitro* evaluations of high knee flexion postures (Thompson et al., 2015).

A variety of high knee flexion postures exist in activities of daily living where intersegmental contact data could be used to improve estimates of mechanical loading exposure. Islamic religious practices and traditional East Asian cultural customs involve symmetric high flexion

kneeling with the feet in dorsiflexion or plantarflexion (Hefzy et al., 1998; Hemmerich et al., 2006). High knee flexion squatting is also common during childcare, sport, and toileting in many cultures (Hemmerich et al., 2006; Kurosaka et al., 2002). Finally, single-leg (unilateral) kneeling is used during many occupational tasks (Gallagher et al., 2011; Pollard et al., 2011) and is a primary shooting position used in military theater (Army, 2010). During symmetric kneeling, thigh-calf contact force has been reported at up to 34% BW (Zelle et al., 2007) with a separate study reporting heel-gluteal contact forces of approximately 11% BW (Pollard et al., 2011). However, only a dorsiflexed foot position was tested during kneeling, and there is no known thigh-calf or heel-gluteal contact data for unilateral kneeling positions. Further investigation of heel-gluteal contact is needed as the large moment arm has resulted in similar knee extension moments to thigh-calf contact with considerably smaller forces (Pollard et al., 2011). Therefore, also including heel-gluteal contact forces in future modelling efforts is needed to improve the biofidelity of tibial compressive loads.

Prior work on thigh-calf contact involved assessment only in the sagittal plane, and pressure sensors were not attached to segments. Small sample sizes (10 participants) prevented the investigation of sex differences in prior work (Pollard et al., 2011; Zelle et al., 2007). Given anthropometric (Power and Schulkin, 2008) and flexibility differences between sexes (Krivickas and Feinberg, 1996), females may be disproportionally exposed to lower joint compressive loads as a result of increased thigh-calf and heel-gluteal contact in high flexion postures. In addition, females generally have a higher distribution of body-fat in the pelvic and thigh region (Cnop et al., 2003; Nielsen et al., 2004) which may also result in different intersegmental loading when compared to males. Past studies have relied on manually positioning, or having participants hold, pressure sensors in place while performing movement trials (Pollard et al., 2011; Zelle et al.,

2007). This reduced repeatability between trials, and did not allow for unilateral postures as larger pressure sensors designed for seating applications (Conformat model #5330, Tekscan, South Boston, MA, USA) were used. Finally, prior studies used sensors with a spatial resolution of 0.5 sensels per cm^2, and were collected at a maximum of 8 Hz (Pollard et al., 2011; Zelle et al., 2007).

Therefore, the purpose of this study was to define the following parameters for thigh-calf and heel-gluteal contact from six high knee flexion postures: 1) knee flexion angle at which thigh-calf contact begins ('onset'), 2) maximum knee flexion range ('max angle'), 3) contact force magnitude ('force'), 4) contact force area ('area'), and 5) longitudinal center of force ('CoF') location. All reported outcomes occurred simultaneously, with the exception of onset. A secondary objective of this study was to investigate sex differences in these outcome parameters.

2. Materials and Methods

2.1. Participants

Twenty-eight male and thirty female participants (Table 1) were recruited from a sample of convenience in the university's student body. Exclusion criteria consisted of any low back, or lower limb injury within the past year that required medical intervention or time off from work for longer than three days, and any history of surgical interventions to the back or lower limb. Only one participant was not right leg dominant. Each participant read and signed an informed consent form approved by the university's research ethics board.

INSERT TABLE 1 ABOUT HERE

2.2. Experimental protocol

Participant height and segmental anthropometrics (Table 1), from the right lower limb, were measured before instrumentation. Participant mass was calculated from force plate data during a static calibration trial. Thigh and shank skinfold measurements were taken at the midpoint between the inguinal fold and the anterior surface of the patella and the most medial aspect of maximal shank girth respectively (International Society for the Advancement of Kinanthropometry, 2001) as a gross representation of adiposity. Thigh length was measured as the distance between the palpated greater trochanter and lateral femoral condyle. Thigh circumference measurements were taken at three distances from the greater trochanter: 10% (proximal), 50% (mid), and 90% (distal) of thigh length. Shank length was measured as the distance between the palpated lateral tibial condyle and malleolus with circumferences measured at the same distances, from the lateral tibial condyle, as the thigh.

Following preparations for kinematic tracking, participants then completed a static standing trial, followed by knee and hip functional joint center trials (Besier et al., 2003; Camomilla et al., 2006). After conditioning (see section 2.2.1), the pressure sensor was then attached to the posterior right thigh (Figure 1). Participants first observed the movements, which were performed by the researcher, and then practiced until they could perform each comfortably. Five repetitions of the following six movements (Figure 2) were completed in a fully randomized order: heels-up squat (HS), flatfoot squat (FS), dorsiflexed kneel (DK), plantarflexed kneel (PK), dorsiflexed unilateral kneel (DUK), and plantarflexed unilateral kneel (PUK). Each trial took 6 seconds to complete and consisted of stepping onto embedded force plates, descending to end range of motion, and statically holding the position. Participants moved at a self-selected speed with movement instructions of: step with the right foot first followed by the left (all movements);

kneel onto the right knee during the transitional phase (Figure 1 – kneeling movements); then assume the final posture (Figure 2). When performing unilateral kneeling movements, participants were instructed to support the majority of their body weight on the right leg in the static hold of these positions similar to techniques used in military theater (Army, 2010).

FIGURE 1 ABOUT HERE

FIGURE 2 ABOUT HERE

2.2.1. Instrumentation

Kinematic data were recorded at 64 Hz from rigid bodies attached to the right thigh, shank, foot, and the pelvis using an optoelectronic system (Certus, NDI, Waterloo, ON). Kinetic data were synchronously recorded at 2048 Hz from four embedded force plates (OR6-7, AMTI, Watertown, MA). Pressure data were synchronously recorded at 64 Hz (3005E-FScan, Tekscan, Boston, MA). This 8-bit resistive pressure sensor had a spatial resolution of 3.9 sensels/cm^2 and a sensing region that was 15.75 cm wide by 39.62 cm long. It was conditioned to 103.4 kPa ten times in 3-second cycles, equilibrated for 30 seconds at three points (34.5 kPa, 68.9 kPa, and 103.4 kPa) then calibrated following the manufacturer's non-linear (power) procedure (Table 3). The power calibration is the most accurate calibration provided in Tekscan software for varying load applications (Brimacombe et al., 2009).

2.3. Data processing

All data processing was completed using Matlab 9.0 (The Mathworks, Release R2016a, Natick, MA). Kinematic and ground reaction force (GRF) data were low-pass filtered using a

bidirectional 2nd-order Butterworth digital filter with a 6 Hz cut-off frequency (Longpré et al., 2013; Winter, 2009). Knee and hip joint centers were calculated from functional trials following established protocols (Besier et al., 2003; Camomilla et al., 2006). Knee joint angles were decomposed following ISB standards in a Z-Y-X Cardan sequence (Wu and Cavanagh, 1995). Data were then truncated, starting when the GRF under the right foot (always the first foot to contact a force plate) exceeded 10N. The trial end point was manually identified as the frame where the knee flexion waveform plateaued. All data were then time normalized and averaged across the five repetitions of each movement.

Raw pressure data, from the last frame of the truncated trial, underwent a 'masking' procedure to identify regions of thigh-calf and heel-gluteal contact for every repetition (Figure 3). Thigh-calf and heel-gluteal masks were represented as matrices of 78 x 31 logical values (1 if element was in selected region, 0 if not) and multiplied by the raw data to omit the values of unselected sensels. This procedure was completed to reduce sensor noise as sensor deformation around the small circumference of the calcaneus resulted in pressure artifacts (Figure 3 – A vs D). Masking was completed on all trials for each participant (900 frames x 2 masks) twice (figure displayed maxima of 30 and 80 kPa) to allow for an intraclass correlation (ICC) of mask selection reliability, and then completed by two additional untrained raters, at 30 kPa, to estimate interrater reliability.

After masking, onset was calculated using knee flexion angle and total force from the pressure sensor. Mean and standard deviation were calculated from force data in a 10-frame window surrounding the frame when the knee flexion angle reached 110º. The onset threshold was defined as the mean plus two standard deviations. Onset (Figure 4 – data at the point of onset indicated by black circles) was defined as the flexion angle at the frame where force data

exceeded this threshold (Hodges and Bui, 1996). Contact area values were calculated from both contact regions as the sum of sensel areas that had values greater than 0 kPa after masking.

INSERT FIGURE 3 HERE

INSERT FIGURE 4 HERE

Longitudinal CoF was calculated as the distance from the functional knee joint center for both the thigh-calf and heel-gluteal contact regions using a weighted-centroid approach (Verkerke et al., 2005). A fixed transformation used to position the pressure sensor (and thus the CoF) with respect to the thigh was defined (Figure 5). Points on the pressure sensor that were digitized in the global coordinate system while the participant was standing upright were used to define a local coordinate system on the sensor, which was assumed to lay flat in the regions where contact occurred. The y-z plane of the sensor was positioned parallel to the frontal plane of the thigh segment. Anterior-posterior positioning of the sensor was accomplished by setting the perpendicular distance between these two planes (A) such that sensor passed through the midpoint (O) of a vector between the most posterior points of the mid-thigh (M) and distal thigh (D) circumferences. The angle between the long axis of the pressure sensor and the long axis of the thigh in the plane of the sensor was then calculated using the dot product to convert CoF points from the sensor coordinate system into the thigh.

2.4. Statistical analyses

To estimate trained rater reliability in mask selection, a two-way random ICC(2,1) was completed for 58 participants, using average absolute agreement between thigh-calf region CoF

from the 30 and 80 kPa rounds of masking (Cicchetti, 1994; Shrout and Fleiss, 1979). Similarly, a second two-way random ICC(2,3) was completed to estimate rater reliability between the trained and two untrained raters in selecting masks. To assess differences between high knee flexion contact parameters across the six postures, a linear mixed model was used with fixed effects of posture and sex, and *a-priori* $\alpha = 0.05$. Dependent variables were onset, max angle, and the following measures taken at the last frame of the truncated trial (max angle): total force, thigh-calf force, thigh-calf CoF, thigh-calf area, heel-gluteal force, heel-gluteal CoF, and heel-gluteal area. Bonferroni corrections were applied for *post-hoc* pairwise comparisons to adjust α levels for multiple comparisons. All statistical analyses were completed using SPSS (IBM Corp. Released 2011. IBM SPSS Statistics for Windows, Version 20.0, Armonk, NY).

3. Results

ICC(2,1) estimates were excellent (lowest value 0.932) between masking attempts at different kPa display levels (Cicchetti, 1994). Likewise, ICC(2,3) values were excellent between raters (lowest single and mean values 0.873 and 0.954 respectively). A complete set of mean values and standard deviations for dependent variables is in Table 2. Notable differences are reported below.

INSERT TABLE 2 ABOUT HERE

3.1. Range of flexion during thigh-calf contact

There was a main effect of posture and sex for both onset ($p < 0.001$ and $p = 0.01$) and max angle (both $p < 0.001$). These two variables define the range of flexion over which thigh-calf contact occurred. For male participants, onset (121.0º) and max angle (147.4º) occurred on

average 3.1º and 7.0º earlier than for females (onset: 124.1º and max angle: 154.4º). Onset occurred earliest in PK (119.7º) which was 8.4º earlier ($p < 0.001$) than the activity with the latest onset, FS (128.1º). The only posture-pair (e.g. squatting, symmetric kneeling, or unilateral kneeling) that had onset differences was unilateral kneeling; PUK (119.9º) had a 4.4º earlier onset ($p < 0.001$) than DUK (124.3º). In addition, the movement with the highest max angle was PK (152.7º) which was 3.2º higher ($p < 0.001$) than the activity with the lowest max angle, FS (149.5º).

3.2. Contact force

For the measured forces, there was a main effect of posture only for total force ($p < 0.001$), thigh-calf force ($p < 0.001$), and heel-gluteal force ($p = 0.012$) at max angle. Individual participant and mean total force curves for each movement (normalized to percent body weight for comparison to previous data) are shown in Figure 6. Only two total force pairwise comparisons (Table 2) were not significantly different: DK vs. PK and DUK vs. PUK ($p = 1.00$ and 0.27 respectively). The range of mean total contact force at max angle was 139.08N, from 51.07N in FS to 190.15N in DUK.

Similar to total force, all thigh-calf contact force pairwise comparisons (Table 2) were different ($p < 0.001$) except for symmetric kneeling (DK and PK, $p = 1.00$). The highest thigh-calf contact force was in DUK (186.76N) which was 135.69N more force than FS (51.07N).

Heel-gluteal contact only occurred for 15 females and 11 males in DUK, 12 females and 11 males in PK, 14 females and 4 males in PUK, and 7 females in DK. Of this sub-sample, heel-gluteal contact force was highest in PUK (23.92N) which was 12.99N higher ($p = 0.02$) than DUK (10.93N) and 17.41N higher ($p = 0.02$) than DK (6.51N).

3.3. Center of force

An interaction was observed for the thigh-calf region CoF ($p = 0.002$). In DUK, the CoF was 15 mm farther from the knee joint center in females when compared to males (82 and 67 mm respectively). A main effect of posture ($p = 0.008$) was present for the heel-gluteal region CoF, with a 19 mm difference ($p = 0.01$) occurring between PUK (316 mm) and DUK (335 mm).

3.4. Contact area

Similar to section 3.3, an interaction was observed for thigh-calf contact area ($p = 0.013$). In DUK, contact area was 18.28 cm^2 larger for females (155.61 cm^2) when compared to males (137.33 cm^2). A main effect of posture ($p = 0.023$) was present for heel-gluteal contact area, with PUK (10.05 cm^2) having a 3.97 cm^2 larger area ($p = 0.022$) than DUK (6.08 cm^2).

4. Discussion

The purpose of this investigation was to define thigh-calf and heel-gluteal contact parameters for six high knee flexion movements and to investigate potential sex differences. Results indicate that unilateral kneeling movements have the highest thigh-calf contact forces occurring at CoF locations farthest from the knee joint center. These activities would therefore theoretically result in the greatest reduction of knee joint flexion moments for the right knee, although not necessarily the lowest joint moment or compression force. Squatting movements had the lowest thigh-calf contact forces, with the majority of participants (35) unable to achieve thigh-calf contact when performing FS. Sex differences occurred in range of flexion parameters (onset and max angle), with males having lower thigh-calf contact onset and max angle. This difference effectively shifts the entire range of flexion during contact to lower flexion angles for males. Interactions of sex by movement occurred whereby sex had a significant effect on contact area

and CoF location for the thigh-calf and heel-gluteal regions for the DUK posture only. It should be noted that our results (specifically sex differences) reported in this study only relate to our sample of healthy, young, non-habitually kneeling participants and the reader is cautioned against generalizing these findings to a population level.

The knee flexion angle where the onset of thigh-calf contact occurred was approximately 10º to 15º earlier than values reported by Zelle et al. (2007), however, our max angles are also approximately 5º lower. This is likely attributed to differences in kinematic tracking as three markers were used to define thigh and shank motion in Zelle et al., (2007), as opposed to 3D reconstruction with functional joint centers (Besier et al., 2003; Camomilla et al., 2006) used in our study. In addition, there is a non-sensing boarder around the perimeter of previously used sensors that may contribute to later onset angles. The sensor used in this study was more sensitive, therefore it enabled the use of onset criterion similar to established methods used in electromyographic work (Hodges and Bui, 1996). This threshold is different from the 5% bodyweight value used by Zelle et al., (2007).

The mean total contact force values reported in this study are considerably lower than prior work (Table 3). However, it should be noted that a small number of participants achieved similar contact force magnitudes in our sample population (Figure 6). While it appears to have been largely ignored in prior work, noise within pressure sensor technology can be considerable when performing high knee flexion movements due to the deformation of the sensor. For example, noise represented 51.9N ≈ 30% of the raw total force displayed in Figure 3A. Also, the approach used to calibrate Tekscan sensors can alter output substantially as the power calibration method (used in the current study) is almost ten times more accurate, across full scale output, when compared to linear methods (Brimacombe et al., 2009). Previous work used linear calibration

methods (Pollard et al., 2011; Zelle et al., 2007). In addition, contact areas were less than 50% of those reported in Zelle et al., (2007) and thus lower total contact forces would be expected. Differences in participant anthropometrics (e.g. thigh circumference/skinfold thickness) likely contributed to the differences in contact areas between these studies, but this theory is speculative as segment circumferences were not reported in previous work. As well, for the same thigh-calf contact area, the finer spatial resolution of the pressure sensor used in the current study would result in a smaller contact area measured, compared to a sensor with coarser resolution. Finally, it should be noted that prior work did not explicity state if participants were barefoot or shod. Performing kneeling movements while shod can alter ankle flexion by up to 8º (Chong et al., 2017) and could result in increased contact area and pressure due to matierial of the shoe extending posteriorly from the heel. These issues, in addition to our study using a masking procedure to reduce noise, may help explain the differences in findings between studies.

TABLE 3 ABOUT HERE

Thigh-calf CoF values for HS are considerably lower in this study (≈5.7 ± 1.7 cm) compared to the findings of Zelle et al., (2007) (16.6 ± 2.64 cm), likely a result of smaller contact area measured. Our DK CoF values are separated into thigh-calf and heel-gluteal components, as opposed to an overall CoF, limiting direct comparison to previous work. The difference in the reference points used to express the CoF locations in previous works—perpendicular distance between the posterior knee and the epicondylar axis (Zelle et al., 2007) or midway between the epicondyles of the femur (Pollard et al., 2011)—highlights that a reporting standard needs to be

established. We feel that expressing the CoF with respect to the functional knee joint centre warrants consideration due to the ubiquity of its use in current 3D modeling (Hicks et al., 2014).

Limitations of this study include the manual selection of contact regions, the inability to account for shear loading or deformation in the pressure sensor, soft-tissue artifact, and the weight distribution instruction for unilateral kneeling. Although ICCs were excellent for the user-defined masks, they are subjective and could influence comparisons between studies. As well, the size of this pressure sensor toward the popliteal fossa may have resulted in not measuring thigh-calf contact data in rare instances, similar to the non-sensing border of rectangular pressure sensors. Current pressure sensing technology remains limited in that shear forces cannot be separated from normal force. In addition, deformation of the sensor (especially in heel-gluteal contact regions) manifests as pressure artifacts. Therefore, our assumption that the sensor was flat between contact areas likely results in systematically over-estimated force values. We acknowledge that soft tissue deformation of the thigh and shank segments is considerable during high knee flexion movements, and that this would affect both the calculation of knee flexion angle and confidence in pressure sensor location. Dual-plane fluoroscopic studies are needed in high knee flexion ranges before quantification of soft-tissue error can be estimated from surface tracking (Cereatti et al., 2017). In addition, the authors are not aware of a verified method for tracking sensor deformation during dynamic activities and future work is needed to establish movement between the pressure sensor and segments. Finally, we instructed participants to support the majority of their bodyweight on the flexed leg during unilateral kneeling. This posture was novel to all participants although commonly used in military populations (Army, 2010). Therefore, results for these postures could be interpreted as 'worst-case' *in-vivo* thigh-calf and heel-gluteal load magnitudes.

5. Conclusion

Our results suggest that thigh-calf and heel-gluteal contact can result in considerable force transfer between the thigh and shank segments during high knee flexion movements. While previous work has quantified these effects at the joint loading level (Pollard et al., 2011; Zelle et al., 2009) future work is required to incorporate thigh-calf contact parameters into a 3D musculoskeletal model (Thompson et al., 2015). It is noteworthy that the population used in this study—consisting of young, generally active participants from many ethnic backgrounds—was largely unable to attain heel-gluteal contact in kneeling postures. Given our findings are markedly lower than previously published values in almost all contact parameters, it seems pertinent to recommend that future work on thigh-calf contact should include detailed information about calibration procedures, instrumentation, and participant anthropometrics to facilitate comparisons between studies. As well, data is needed from sufficiently sampled populations with specific cultural or occupational kneeling practices that are linked to increased risks of knee joint degenerative diseases.

Acknowledgements

We would like to acknowledge that SM Acker is funded through an NSERC Discovery Grant #418647. This funding source was not involved with study implementation or submission.

Conflict of interest

The authors have no financial and personal relationships with other people or organizations that could inappropriately influence their work.

6. References

Andriacchi, T.P., Favre, J., 2014. The Nature of In Vivo Mechanical Signals That Influence Cartilage Health and Progression to Knee Osteoarthritis. Curr. Rheumatol. Rep. 16, 1–8. doi:10.1007/s11926-014-0463-2

Andriacchi, T.P., Mündermann, A., Smith, R.L., Alexander, E.J., Dyrby, C.O., Koo, S., 2004. A framework for the in vivo pathomechanics of osteoarthritis at the knee. Ann. Biomed. Eng. 32, 447–57.

Army, D. of the, 2010. Technical Manual No. 3-22.31.

Baker, P., Reading, I., Cooper, C., Coggon, D., 2003. Knee disorders in the general population and their relation to occupation. Occup. Environ. Med. 60, 794–797. doi:10.1136/oem.60.10.794

Besier, T., Sturnieks, D., Alderson, J., Lloyd, D., 2003. Repeatability of gait data using a functional hip joint centre and a mean helical knee axis. J. Biomech. 36, 1159–1168. doi:10.1016/S0021-9290(03)00087-3

Bombardier, C., Hawker, G., Mosher, D., 2011. the Impact of Arthritis in Canada: Today and Over the Next 30 Years. Arthritis Alliance of Canada.

Brimacombe, J.M., Wilson, D.R., Hodgson, A.J., Ho, K.C.T., Anglin, C., 2009. Effect of Calibration Method on Tekscan Sensor Accuracy. J. Biomech. Eng. 131, 34503. doi:10.1115/1.3005165

Camomilla, V., Cereatti, A., Vannozzi, G., Cappozzo, A., 2006. An optimized protocol for hip joint centre determination using the functional method. J. Biomech. 39, 1096–106. doi:10.1016/j.jbiomech.2005.02.008

Cereatti, A., Bonci, T., Akbarshahi, M., Aminian, K., Barré, A., Begon, M., Benoit, D.L.,

Charbonnier, C., Maso, F.D., Fantozzi, S., Lin, C.-C., Lu, T.-W., Pandy, M.G., Stagni, R., van den Bogert, A.J., Camomilla, V., 2017. Standardization proposal of soft tissue artefact description for data sharing in human motion measurements. J. Biomech. doi:10.1016/j.jbiomech.2017.02.004

Chong, H.C., Tennant, L.M., Kingston, D.C., Acker, S.M., 2017. Knee joint moments during high flexion movements: Timing of peak moments and the effect of safety footwear. Knee 24, 271–279. doi:10.1016/j.knee.2016.12.006

Cicchetti, D., 1994. Guidelines, criteria, and rules of thumb for evaluating normed and standardized assessment instruments in psychology. Psychol. Assess. 6, 284–290. doi:10.1037/1040-3590.6.4.284

Cnop, M., Havel, P.J., Utzschneider, K.M., Carr, D.B., Sinha, M.K., Boyko, E.J., Retzlaff, B.M., Knopp, R.H., Brunzell, J.D., Kahn, S.E., 2003. Relationship of adiponectin to body fat distribution, insulin sensitivity and plasma lipoproteins: evidence for independent roles of age and sex. Diabetologia 46, 459–469. doi:10.1007/s00125-003-1074-z

Gallagher, S., Pollard, J., Porter, W.L., 2011. Electromyography of the thigh muscles during lifting tasks in kneeling and squatting postures. Ergonomics 54, 91–102. doi:10.1080/00140139.2010.535025

Hefzy, M.S., Kelly, B.P., Cooke, T.D., 1998. Kinematics of the knee joint in deep flexion: a radiographic assessment. Med. Eng. Phys. 20, 302–7.

Hemmerich, A., Brown, H., Smith, S., Marthandam, K., Wyss, U., 2006. Hip, Knee, and Ankle Kinematics of High Range of Motion Activities. J. Orthop. Res. 24, 770–781. doi:10.1002/jor.20114

Hicks, J.L., Uchida, T.K., Seth, a, Rajagopal, a, Delp, S., 2014. Is my model good enough? Best

practices for verification and validation of musculoskeletal models and simulations of human movement. J. Biomech. Eng. 137. doi:10.1115/1.4029304

Hodges, P.W., Bui, B.H., 1996. A comparison of computer-based methods for the determination of onset of muscle contraction using electromyography. Electroencephalogr. Clin. Neurophysiol. 101, 511–519. doi:10.1016/S0921-884X(96)95190-5

Hofer, J., Gejo, R., McGarry, M., Lee, T., 2012. Effects of kneeling on tibiofemoral contact pressure and area in posterior cruciate-retaining and posterior cruciate-sacrificing total knee arthroplasty. J. Arthroplasty 27, 620–4. doi:10.1016/j.arth.2011.07.011

International Society for the Advancement of Kinanthropometry, 2001. International Standards for Anthropometric Assessment. The international society for the advancement of kinanthropometry, Underdale, AUS.

Kingston, D.C., Tennant, L.M., Chong, H.C., Acker, S.M., 2016. Peak activation of lower limb musculature during high flexion kneeling and transitional movements. Ergonomics 139, 1–9. doi:10.1080/00140139.2015.1130861

Kirkeshov Jensen, L., 2008. Knee osteoarthritis: influence of work involving heavy lifting, kneeling, climbing stairs or ladders, or kneeling/squatting combined with heavy lifting. Occup. Environ. Med. 65, 72–89. doi:10.1136/oem.2007.032466

Krivickas, L.S., Feinberg, J.H., 1996. Lower extremity injuries in college athletes: Relation between ligamentous laxity and lower extremity muscle tightness. Arch. Phys. Med. Rehabil. 77, 1139–1143. doi:10.1016/S0003-9993(96)90137-9

Kurosaka, M., Yoshiya, S., Mizuno, K., Yamamoto, T., 2002. Maximizing flexion after total knee arthroplasty: the need and the pitfalls. J. Arthroplasty 17, 59–62. doi:10.1054/arth.2002.32688

Longpré, H., Potvin, J., Maly, M., 2013. Biomechanical changes at the knee after lower limb fatigue in healthy young women. Clin. Biomech. 28, 441–7. doi:10.1016/j.clinbiomech.2013.02.010

Nielsen, S., Guo, Z., Johnson, C.M., Hensrud, D.D., Jensen, M.D., 2004. Splanchnic lipolysis in human obesity. J. Clin. Invest. 113, 1582–1588. doi:10.1172/JCI200421047

Pollard, J.P., Porter, W.L., Redfern, M.S., 2011. Forces and moments on the knee during kneeling and squatting. J. Appl. Biomech. 27, 233–41.

Power, M.L., Schulkin, J., 2008. Sex differences in fat storage, fat metabolism, and the health risks from obesity: possible evolutionary origins. Br. J. Nutr. 99, 931–940. doi:10.1017/S0007114507853347

Shrout, P.E., Fleiss, J.L., 1979. Intraclass correlations: Uses in assessing rater reliability. Psychol. Bull. 86, 420–428. doi:10.1037/0033-2909.86.2.420

Thompson, W.K., Gallo, C.A., Crentsil, L., Lewandowski, B.E., Humphreys, B.T., Dewitt, J.K., Fincke, R.S., 2015. Digital Astronaut Project Biomechanical Models Biomechanical Modeling of Squat , Single-Leg Squat and Heel Raise Exercises on the Hybrid Ultimate Lifting Kit (HULK). Hampton, VA.

Verkerke, G.J., Hof, A.L., Zijlstra, W., Ament, W., Rakhorst, G., 2005. Determining the centre of pressure during walking and running using an instrumented treadmill. J. Biomech. 38, 1881–1885. doi:10.1016/j.jbiomech.2004.08.015

Victor, J., Van Glabbeek, F., Vander Sloten, J., Parizel, P.M., Somville, J., Bellemans, J., 2009. An experimental model for kinematic analysis of the knee. J. bone Jt. Surg. 91 Suppl 6, 150–163. doi:10.2106/JBJS.I.00498

Winter, D., 2009. Biomoechanics and Motor Control of Human Movement, 4th ed. John Wiley

& Sons, Inc., Hoboken.

Wu, G., Cavanagh, P., 1995. ISB recommendations for standardization in the reporting of kinematic data. J. Biomech. 28, 1257–1261.

Zelle, J., Barink, M., De Waal Malefijt, M., Verdonschot, N., 2009. Thigh-calf contact: Does it affect the loading of the knee in the high-flexion range? J. Biomech. 42, 587–593. doi:10.1016/j.jbiomech.2008.12.015

Zelle, J., Barink, M., Loeffen, R., De Waal Malefijt, M., Verdonschot, N., 2007. Thigh-calf contact force measurements in deep knee flexion. Clin. Biomech. 22, 821–826. doi:10.1016/j.clinbiomech.2007.03.009

Figure 1: Participant performing a transition to kneeling with the Tekscan (3005E) sensor attached to the posterior thigh and positioned so the edge closest to the knee joint entered the popliteal fossa upon flexion.

Figure 2: High knee flexion postures performed in this study: 1) Heels-up squat (top left), 2) flatfoot squat (bottom left), 3) dorsiflexed kneel (top middle), D) plantarflexed kneel (bottom middle), E) dorsiflexed unilateral kneel (top right), and F) plantarflexed unilateral kneel (bottom right).

Figure 3: Raw (A) to masked (D) Tekscan sensor data completed through regional selections using a custom Matlab function. The frame of Tekscan data at Max Angle for every repetition was used to define masks for the thigh-calf and heel-gluteal (if applicable) contact regions. A is the raw data, B is the selection of thigh-calf contact mask, C is the selection of heel-gluteal mask with an arrow pointing to the region for clarity, and D is the masked data where raw data is multiplied by a logical matrix (1 if element was in selected region, 0 if not) to omit the values of

unselected sensels. For this example: total force in A = 175.4N; total force in D = 123.5N (51.9N difference from A); thigh-calf force in D = 87.7N; heel-gluteal force = 35.8N.

Figure 4: Thigh-calf contact onset criteria. The vertical dashed lines indicate a window of 10 data points surrounding the frame in which the participant reached 110º of knee flexion. The mean (bottom of shaded region) and standard deviation of the force values in this window were used to define the onset threshold (top of the shaded region at 2 SD above the mean). The circled red point indicates where force data exceeded onset threshold and the circled blue point indicates the knee flexion angle where onset of thigh-calf contact occurred.

Figure 5: Sagittal view of the femur and shank depicting the position of the pressure sensor plane (hashed black rectangle) referenced to the thigh segment. Point M (green circle) is the posterior point on the mid-thigh circumference located at 50% of segment length. Point D (green circle) is the posterior point on the distal thigh circumference located at 90% of segment length. Point O (red X) is the mid-point between points M and D, which was used to define the anterior-posterior position of the Tekscan sensor that was a fixed perpendicular distance (A) from the long axis of the femur (vertical black arrow).

Figure 6: Participant (grey) and mean (red) with shaded ± 1 SD band total force values across movements. Percentage movement after contact represents the time from onset to max angle for each participant.

Table 1: Mean (standard deviation) descriptive and anthropometric participant information.

Table 2: Mean values (± 1 SD) of high knee flexion parameters. † and ‡ indicate main effects of posture or sex respectively, * indicates an interaction of posture and sex (differences occurred in the DUK posture only). Values sharing lettered superscripts are not different within a column. HS is heels-up squat, FS is flatfoot squat, DK is dorsiflexed kneel, PK is plantarflexed kneel, DUK is dorsiflexed unilateral kneel, and PUK is plantarflexed unilateral kneel. TC is thigh-calf and HG is heel-gluteal contact. CoF is center of force.

Table 3: Summary of thigh-calf contact methods and findings from in vivo studies. All sensor models are from Tekscan (Tekscan Inc., South Boston, MA, USA). Mean (SD) contact force values are reported for the Heels-Up and Dorsiflexed Kneeling movements consistent across the listed studies. Dorsiflexed kneel values from Pollard et al., (2011) and the current study are reported with thigh-calf (left) and heel-gluteal (right) segregated values.

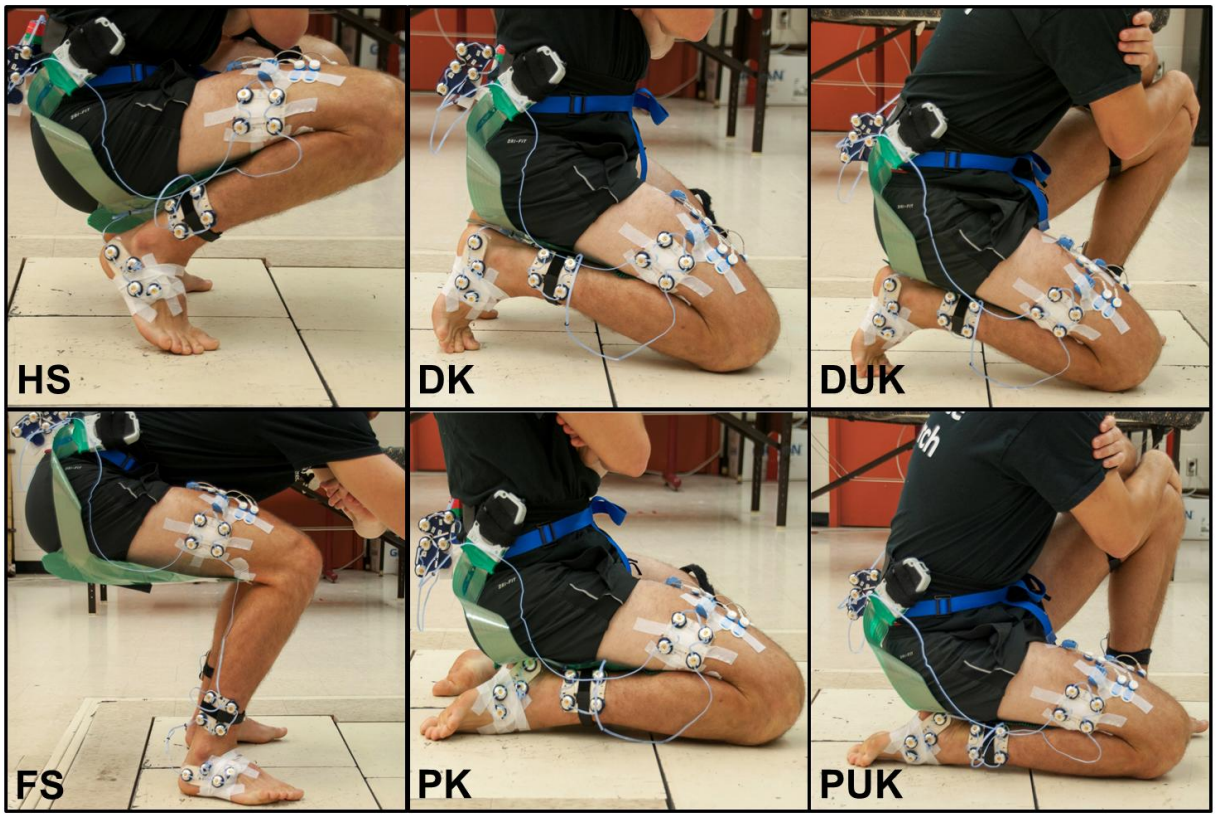

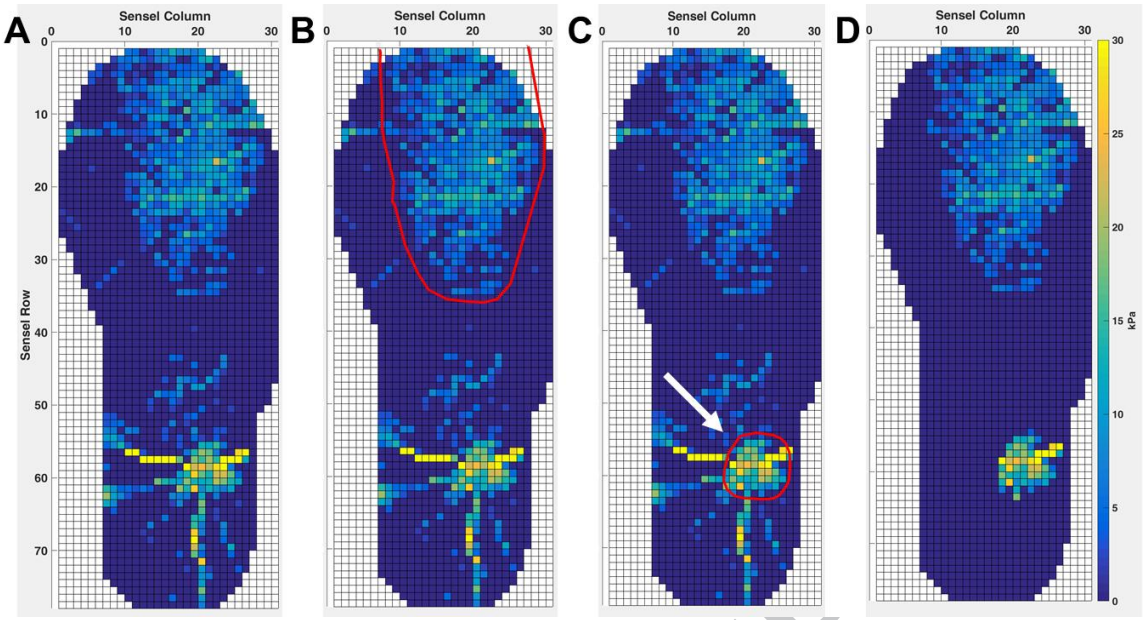

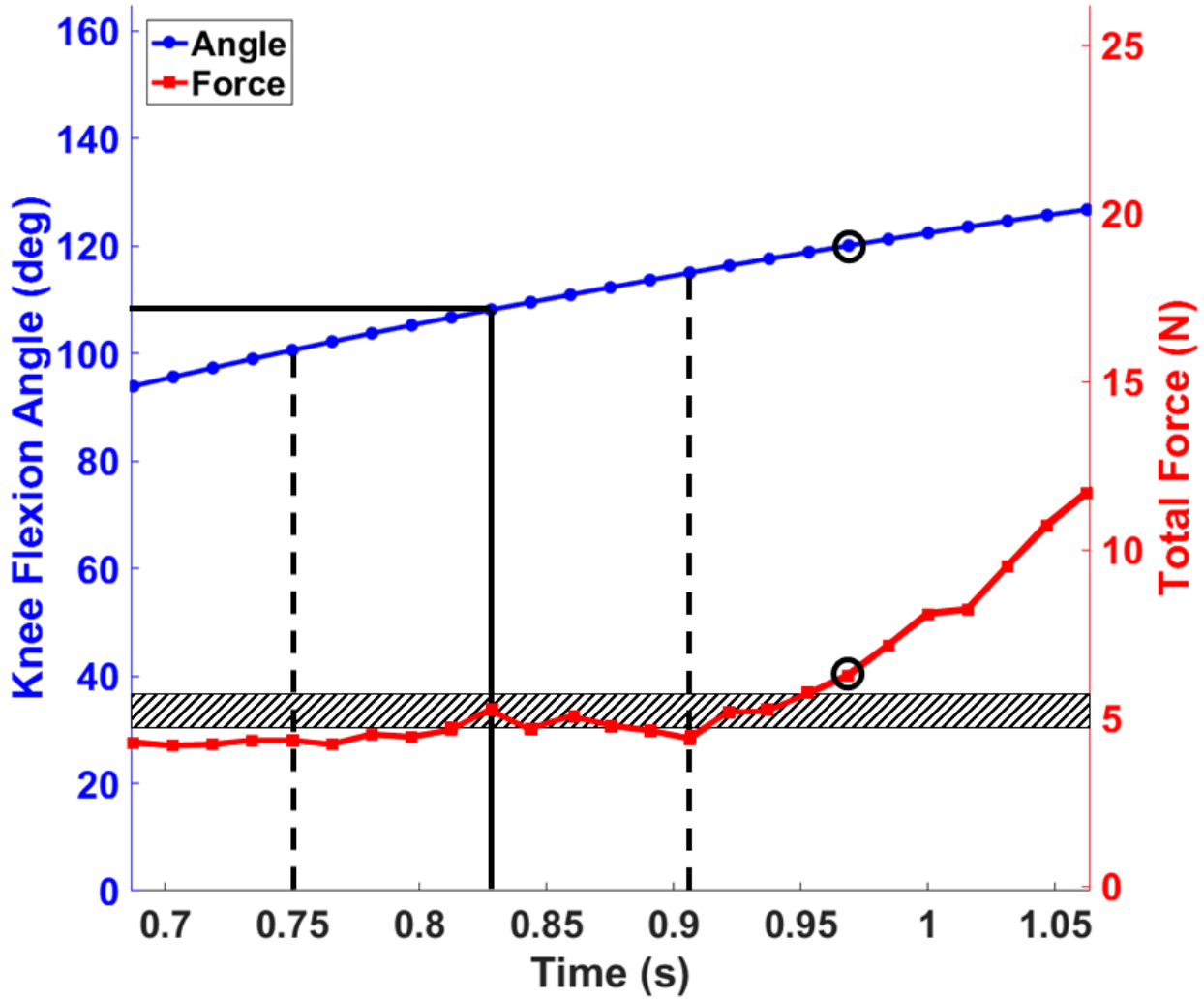
Angle
Force
Knee Flexion Angle (deg)
Total Force (N)
Time (s)
160
140
120
100
80
60
40
20
0
25
20
15
10
5
0
0.7
0.75
0.8
0.85
0.9
0.95
1
1.05

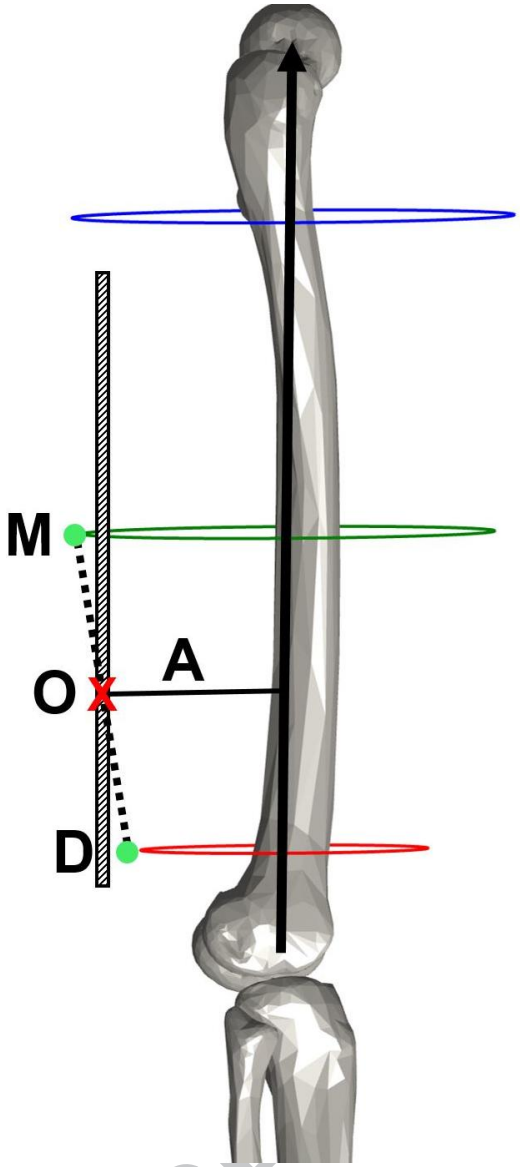

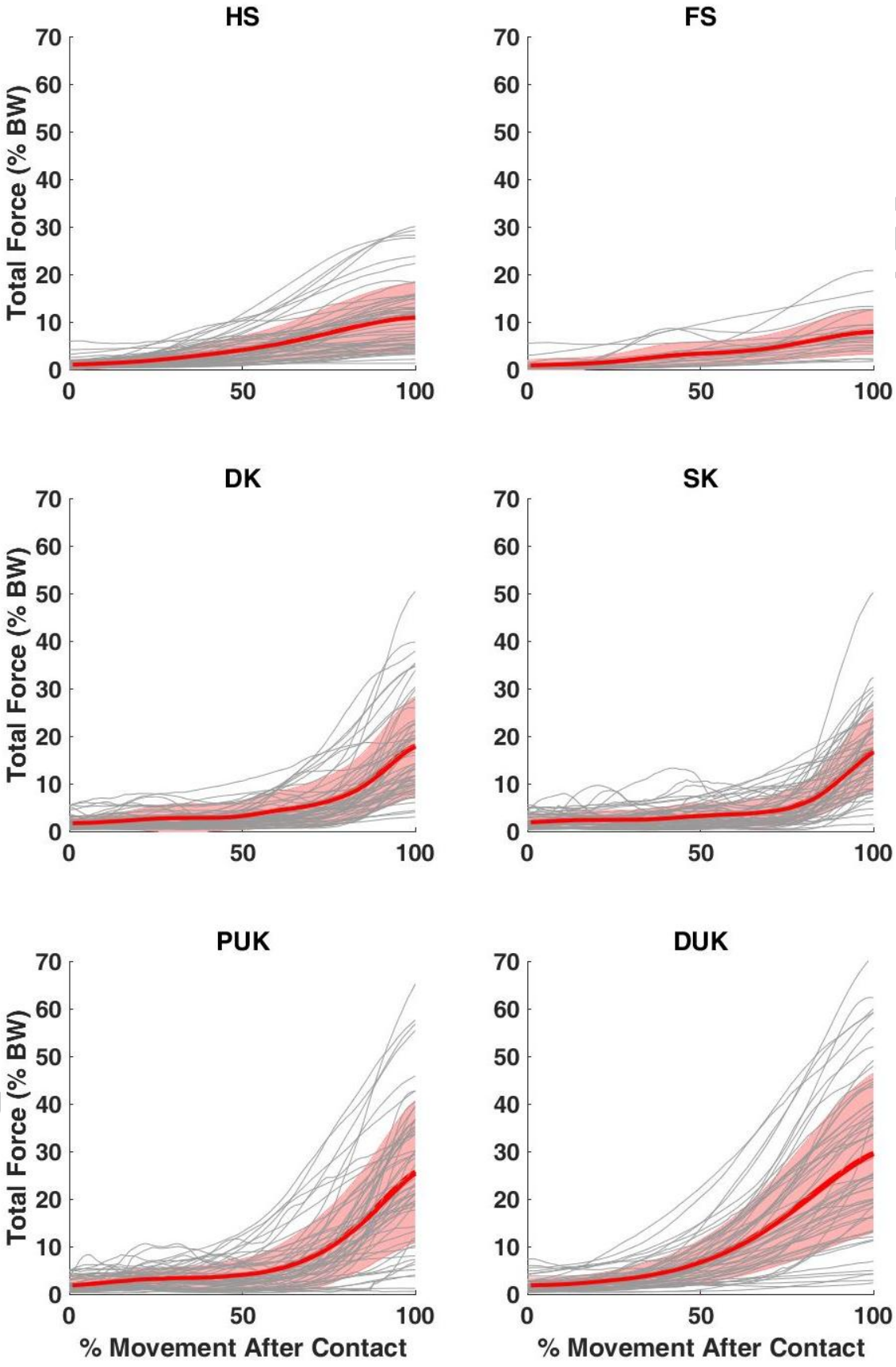
HS
FS
DK
SK
PUK
DUK
Total Force (% BW)
% Movement After Contact
0
10
20
30
40
50
60
70
0
50
100

Table 1 – Mean (standard deviation) descriptive and anthropometric participant information.

Parameter	Female (*n* = 30)	Male (*n* = 28)	Total (*n* = 58)
Age (yrs)	21.0 (3.8)	23.7 (3.8)	22.33 (4.0)
Height (m)	1.63 (0.06)	1.77 (0.07)	1.70 (0.10)
Mass (kg)	61.67 (10.26)	77.15 (15.60)	69.15 (15.15)
BMI (kg/m^2)	23.25 (3.84)	24.57 (4.08)	23.89 (3.98)
Thigh Length (m)	0.39 (0.05)	0.40 (0.03)	0.40 (0.04)
Proximal Thigh Circumference (m)	0.56 (0.06)	0.58 (0.08)	0.57 (0.07)
Mid-Thigh Circumference (m)	0.51 (0.06)	0.54 (0.08)	0.52 (0.07)
Distal Thigh Circumference (m)	0.39 (0.05)	0.40 (0.03)	0.40 (0.04)
Thigh Skinfold (mm)	32 (12)	19 (13)	26 (14)
Shank Length (m)	0.37 (0.03)	0.40 (0.03)	0.39 (0.03)
Proximal Shank Circumference (m)	0.33 (0.03)	0.34 (0.03)	0.33 (0.03)
Mid Shank Circumference (m)	0.34 (0.03)	0.37 (0.04)	0.36 (0.04)
Distal Shank Circumference (m)	0.20 (0.02)	0.22 (0.02)	0.21 (0.02)
Shank Skinfold (mm)	18 (11)	13 (12)	16 (11)

Table 2: Mean values (± 1 SD) of high knee flexion parameters. † and ‡ indicate main effects of posture or sex respectively, * indicates an interaction of posture and sex (differences occurred in the DUK posture only). Values sharing lettered superscripts are not different within a column. HS is heels-up squat, FS is flatfoot squat, DK is dorsiflexed kneel, PK is plantarflexed kneel, DUK is dorsiflexed unilateral kneel, and PUK is plantarflexed unilateral kneel. TC is thigh-calf and HG is heel-gluteal contact. CoF is center of force.

Posture	Group	Onset†‡ (deg)	Max Angle†‡ (deg)	Total Force† (N)	TC Force† (N)	TC CoF†* (mm)	TC Area†* (cm^2)	HG Force† (N)	HG CoF† (mm)	HG Area† (cm^2)
HS	Female	126.0 (7.9)	153.0 (7.3)	68.47 (34.86)	68.47 (34.86)	60 (15)	92.14 (26.20)	–	–	–
	Male	123.9 (7.2)	146.2 (9.4)	78.91 (69.13)	78.91 (69.13)	54 (19)	88.79 (36.19)	–	–	–
	Total	125.0 (7.5) [a,b]	149.6 (9.0) [a]	73.59 (54.19)	73.59 (54.19)	57 (17) [a]	90.49 (31.25)	–	–	–
FS[1]	Female	130.6 (9.0)	152.8 (6.6)	42.54 (19.01)	42.54 (19.01)	58 (15)	75.75 (20.65)	–	–	–
	Male	125.5 (5.0)	145.9 (7.1)	60.37 (45.49)	60.37 (45.49)	48 (18)	78.51 (35.88)	–	–	–
	Total	128.1 (7.7) [a]	149.5 (7.5)	51.07 (34.70)	51.07 (34.70)	53 (17)	77.07 (28.29)	–	–	–
DK[2]	Female	124.1 (7.4)	155.2 (7.5)	114.88 (55.17)	113.36 (55.09)	71 (21)	121.57 (36.73)	6.51 (6.17)	343 (18)	3.93 (2.37)
	Male	119.9 (6.5)	148.2 (10.4)	122.65 (80.60)	122.34 (80.55)	63 (19)	120.98 (38.91)	–	–	–
	Total	122.1 (7.3) [b,c,d]	151.8 (9.6) [b,c]	118.63 (68.13) [a]	117.69 (68.11) [a]	67 (20) [b]	121.29 (37.47) [a]	6.51 (6.17) [a]	343 (18) [a,b]	3.93 (2.37)
PK[3]	Female	121.1 (6.4)	156.0 (6.9)	105.16 (49.56)	99.44 (49.00)	62 (15)	110.92 (30.11)	14.28 (9.88)	306 (16)	8.44 (4.43)
	Male	118.2 (6.2)	149.2 (9.2)	123.88 (72.74)	118.98 (68.80)	61 (20)	120.43 (38.51)	12.48 (12.52)	326 (22)	8.91 (4.94)
	Total	119.7 (6.4) [c]	152.7 (8.8) [b]	114.20 (62.01) [a]	108.88 (59.67) [a]	62 (17) [a]	115.51 (34.45) [a]	13.42 (11.00) [a]	315 (22) [a]	8.67 (4.58)
DUK[4]	Female	125.9 (6.9)	155.3 (7.1)	201.49 (89.16)	196.28 (87.66)	82 (27)	155.61 (41.03)	11.17 (11.91)	333 (24)	5.81 (3.89)
	Male	122.7 (8.5)	147.2 (11.9)	178.00 (110.30)	176.56 (109.07)	67 (22)	137.33 (51.10)	10.11 (4.33)	340 (20)	7.01 (3.16)
	Total	124.3 (7.8) [a]	151.4 (10.4) [a,b]	190.15 (99.74) [b]	186.76 (98.20)	75 (26) [b]	146.78 (46.67)	10.93 (10.58) [a]	335 (23) [b]	6.08 (3.68)
PUK[5]	Female	121.0 (6.0)	152.9 (7.5)	167.54 (94.43)	155.34 (92.06)	60 (18)	121.24 (40.88)	24.39 (23.24)	306 (20)	9.67 (4.73)
	Male	118.8 (6.9)	146.7 (12.3)	171.44 (106.28)	162.30 (101.31)	60 (23)	127.92 (48.82)	23.27 (19.57)	330 (21)	10.56 (4.94)
	Total	119.9 (6.5) [d]	149.9 (10.5) [a,c]	169.42 (99.46) [b]	158.70 (95.84)	60 (20) [a]	124.46 (44.61) [a]	23.92 (21.35)	316 (23) [a]	10.05 (4.75)

[1] Only 12 females and 11 males could achieve thigh-calf contact when performing the FS movement.
[2] HG values in DK had 7 females.
[3] HG values in PK had 12 females and 11 males.
[4] HG values in DUK had 15 females and 11 males.
[5] HG values in PUK had 14 females and 4 males.

Table 3: Summary of thigh-calf contact methods and findings from *in vivo* studies. All sensor models are from Tekscan (Tekscan Inc., South Boston, MA, USA). Mean (SD) contact force values are reported for the Heels-Up and Dorsiflexed Kneeling movements consistent across the listed studies. Dorsiflexed kneel values from Pollard et al., (2011) and the current study are reported with thigh-calf (left) and heel-gluteal (right) segregated values.

Study	Participants		Sensor					Heels-Up Squat (%BW)	Dorsiflexed Kneel (%BW)	
	Male	Female	Model	Spatial Accuracy (sensels/cm^2)	Calibration	Sample Rate (Hz)	Sensitivity (kPa)			
Zelle et al., (2007)	8	2	Conformat (model 5330)	0.5	Linear	8	0-33.3	34.2 (9.69)	30.9 (9.31)	
Pollard et al., (2011)	7	3	ClinSeat (model 5315)	1.0	Linear	4	41-207[2] 0-207[2]	39 (14)	28 (13)	11 (6)
Kingston & Acker (2017)	28	30	3005E	3.9	Power[1]	64	0-154[3]	10.98 (7.01)	17.88 (10.14)	1.13 (0.84)

[1] Point 1 – 22.72kg over ≈610 sensels, Point 2 – 114.94kg over ≈820 sensels, Exponent 0.87-1.27, Scaling Factor 0.502-0.84, Sensel Excitation (S) = 34.

[2] Pollard et al., (2011) report a 0-30 PSI range for their sensor, however, details available from the 5315 specification sheet note a 6-30 PSI sensitivity range.

[3] Specifications of the 3005E sensor state a 0-75 PSI or 0-120 PSI sensitivity range, but our F-Scan software allowed changing the excitation voltage of the sensor to lower the effective sensitivity range to ≈0-22 PSI.